LES-CMC SIMULATIONS OF A TURBULENT LIFTED HYDROGEN FLAME IN VITIATED CO-FLOW

by

Ivana STANKOVIĆ* and Bart MERCI

Department of Flow, Heat, and Combustion Mechanics, Ghent University, Ghent, Belgium

Original scientific paper
DOI: 10.2298/TSCI120704035S

Results from a study of turbulent lifted jet flame with conditional moment closure turbulent combustion model are reported. First, a qualitative description of the simulation results is given, by examining the instantaneous resolved species mass fraction fields. The structure of the lifted flame is also assessed by comparing the measured temperature and species mass fraction profiles and the simulation results. The model is able to capture the axial and radial profiles of mixture fraction, temperature and major species. The sensitivity of prediction to boundary conditions is also explored and the lift-off height is found to be very sensitive to the co-flow temperature. Finally, the stabilisation mechanisms, auto-ignition or premixed flame propagation, are addressed. No evidence of premixed flame propagation is found: the diffusion in physical space is negligible for all studied conditions.

Key words: *large eddy simulation, conditional moment closure, lifted flames*

Introduction

The flame under study is a turbulent lifted jet flame of hydrogen, diluted with nitrogen, issuing into a wide co-flow of vitiated air [1, 2]. Lifted flames are a challenging problem since the flame at its base is unstable and involves a significant degree of interactions between chemical and flow time-scales and can be found in number of industrial applications (burners and gas turbines). The interactions between chemical and flow time-scales influence stabilization mechanism of these flames which may stabilize at the certain distance from the nozzle or may propagate and stabilize at the nozzle. The simple burner geometry developed by Cabra and Dibble [1] and Cabra *et al*. [2] at Berkeley University, provides a good base for studying these complex lifted flames and turbulence-chemistry interactions. The conditions that are encountered in furnaces or gas turbine combustion chambers, where there is a re-circulation of hot combustion products which contributes to flame stabilization downstream of the injection, are simulated by this burner. Therefore, the burner configuration allows investigation of stabilization mechanisms for lifted flames environments that are relevant to practical combustion applications. Two stabilization mechanisms can be suggested: auto-ignition and premixed flame propagation. In the experiments, the lift-off distance was very sensitive to small changes in the vitiated co-flow temperature. This sensitivity is a challenging modelling problem for numerical calculations.

Earlier calculations of this flame, have been done within the RANS framework using PDF techniques [2-6], using the eddy dissipation concept [2, 7] and conditional moment closure (CMC) [8]. Large eddy simulation (LES) of this flame has been also performed [9-11]. Good

* Corresponding author; e-mail Ivana.Stankovic@UGent.be

agreement between experimental and computational results has been achieved in several studies. However, current views on the stabilization mechanism of this flame appear to be divergent.

In this paper, the LES-CMC methodology is applied using a detailed reaction mechanism [12]. The aim is to validate the approach for a lifted flame where turbulence-chemistry interactions are of great importance and to discuss flame stabilization.

LES-CMC formulation

The governing equations for the LES are obtained by applying the filtering operation to the instantaneous balance equations. The filtered equations for mass, momentum and a conserved scalar, mixture fraction (ξ) are solved. Details of the LES as applied, are found in [13]. The sub-grid scale stress tensor is modelled by constant Smagorinsky model with the model constant $C_S = 0.1$ and a turbulent Schmidt number $Sc_t = 0.7$ is used. The mixture fraction variance ($\widetilde{\xi''^2}$) is obtained from a gradient type model [14].

CMC is an advance turbulent reacting flow method that attempts to close problem of the turbulence-chemistry interactions. The CMC originates in the hypothesis that most of the fluctuations in the scalar quantities of interest can often be associated with the fluctuations of the only one quantity, mixture fraction. This means that the transport equations are solved for the conditionally filtered reactive scalars, the conditioning being on the mixture fraction. The CMC equations for the conditionally filtered reactive scalars in LES context read [13, 15]:

$$\frac{\partial Q_\alpha}{\partial t} + \underbrace{\widetilde{u_i|\eta}\frac{\partial Q_\alpha}{\partial x_i}}_{T_1} - \underbrace{\widetilde{N|\eta}\ \frac{\partial^2 Q_\alpha}{\partial \eta^2}}_{T_2} = \underbrace{\widetilde{W_\alpha|\eta}}_{T_3} + \underbrace{\frac{1}{\overline{\rho}\widetilde{P}(\eta)}\frac{\partial}{\partial x_i}\left[\overline{\rho}\widetilde{P}(\eta)D_t\frac{\partial Q_\alpha}{\partial x_i}\right]}_{T_4} \tag{1}$$

$$\frac{\partial Q_T}{\partial t} + \underbrace{\widetilde{u_i|\eta}\frac{\partial Q_T}{\partial x_i}}_{T_1} - \underbrace{\widetilde{N|\eta}\left[\frac{1}{c_{p_\eta}}\left(\frac{\partial c_{p_\eta}}{\partial \eta} + \sum_{\alpha=1}^{n} c_{p,\alpha_\eta}\frac{\partial Q_\alpha}{\partial \eta}\right)\frac{\partial Q_T}{\partial \eta} + \frac{\partial^2 Q_T}{\partial \eta^2}\right]}_{T_2} =$$

$$= \underbrace{-\frac{1}{c_{p_\eta}}\sum_{\alpha=1}^{n}\widetilde{h_\alpha W_\alpha|\eta}}_{T_3} + \underbrace{\frac{1}{\overline{\rho}\widetilde{P}(\eta)}\frac{\partial}{\partial x_i}\left[\overline{\rho}\widetilde{P}(\eta)D_t\frac{\partial Q_T}{\partial x_i}\right]}_{T_4} \tag{2}$$

where $Q_\alpha = \widetilde{Y_\alpha|\eta}$ represents the conditionally filtered reactive scalar, $\widetilde{u_i|\eta}$ – the conditionally filtered velocity, and $\widetilde{N|\eta}$ – the conditionally filtered scalar dissipation rate. The variable η is the sample space variable for mixture fraction, ξ, and the operator $|\eta$ denotes fulfilment of the condition on the right hand side of the vertical bar. D_t is the sub-grid scale turbulent diffusivity.

The first term on the left-hand side of eqs. (1) and (2) is the unsteady term. The second term represents the transport by convection (T_1). The last term on the left-hand (T_2) side represents diffusion in mixture fraction space, also known as the conditional scalar dissipation rate term. The first term on the right-hand side (T_3) is the conditional chemical source term, determined using first order closure. The last term on the right-hand side, *i. e.* the sub-grid scale conditional flux (term T_4), accounts for the conditional transport in physical space and it is modelled using the gradient approach. Note that radiation is not accounted for in eq. (2), since radiation is not essential for the study at hand, focusing on the flame base and flame lift-off height, where temperatures are low.

The conditionally filtered velocity is modelled using the assumption that the conditional velocity is equal to unconditional velocity for entire mixture fraction range. For the condi-

tionally filtered scalar dissipation rate, the amplitude mapping closure (AMC) model [16] is used. This model requires an unconditional filtered scalar dissipation rate, modelled as:

$$\widetilde{N} = (D + D_{\mathrm{t}}) \frac{\partial \widetilde{\xi}}{\partial x_{\mathrm{k}}} \frac{\partial \widetilde{\xi}}{\partial x_{\mathrm{k}}} \tag{3}$$

The diffusivity are $D = \nu/\mathrm{Sc}$ and $D_{\mathrm{t}} = \nu/\mathrm{Sc}_{\mathrm{t}}$, where a constant Schmidt number $\mathrm{Sc} = \mathrm{Sc}_{\mathrm{t}} = 0.7$ is used. The unconditional and conditional filtered values are related by:

$$\widetilde{Y}_{\alpha} = \int_0^1 \widetilde{Y_{\alpha} | \eta} \, \widetilde{P}(\eta) \mathrm{d}\eta \tag{4}$$

The density-weighted filtered (FDF) $\widetilde{P}(\eta)$, is assumed to have a β-shape and is calculated from the resolved mixture fraction and its variance.

In LES-CMC methodology it is common practice to solve the CMC equations on a coarser mesh [13, 15, 17]. As the CMC equations require flow-field information obtained from the LES (mixture fraction, velocity, scalar dissipation rate, and diffusivity), an averaging procedure has to be used. The information transfer is done in two steps. First, the averaging procedure must be set for transferring the necessary information from the fine LES mesh to the coarser CMC mesh. Since the LES solver provides unconditional quantities, the model is applied to transform unconditional quantities to conditional ones. Volume averaging is used to calculate unconditional scalars in the CMC resolution as:

$$\widetilde{\psi}^{*} = \frac{\int \widetilde{\psi} \overline{\rho} \mathrm{d}V}{\int \overline{\rho} \mathrm{d}V} \tag{5}$$

where $\widetilde{\psi}^{*} = \widetilde{\xi}^{*}, \widetilde{N}^{*}, \widetilde{u}_i^{*}$ or D_{t}^{*} are the integrated scalars on CMC resolution and $\widetilde{\psi} = \widetilde{\xi}, \widetilde{N}, \widetilde{u}_i$ or D_{t} are calculated in LES. The AMC model is applied at the CMC resolution.

Experimental configuration

The Berkeley burner consists of a fuel jet nozzle and a surrounding perforated disk. The outer disk has a diameter of 210 mm with an 87% blockage and consists of 2200 holes with a diameter of 1.58 mm. An exit collar is surrounding the perforated disk to prevent entrainment of ambient air into the co-flow. The central jet extends 70 mm above the surface of the perforated disk. At this downstream location the co-flow properties are uniform. The stoichiometric mixture fraction (η_{st}) is 0.474. Table 1 summarizes the boundary conditions, where X denotes species mole fraction.

Table 1. Boundary conditions [1-3]

Item	Diameter, [mm]	Velocity, [ms^{-1}]	Temperature, [K]	$X_{\mathrm{H_2}}$[–]	$X_{\mathrm{O_2}}$[–]	$X_{\mathrm{N_2}}$[–]	$X_{\mathrm{H_2O}}$[–]
Co-flow	210	3.5	1045	0.0005	0.1474	0.7534	0.0989
Fuel jet	4.57	107	305	0.2537	0.0021	0.7427	0.0015

The flame spontaneously ignited in the laboratory starting at the downstream locations when the co-flow is operating and the jet flow is turned on. For these conditions, the observed lift-off height was about ten nozzle diameters [2]. There were no visually obvious auto-ignition events well below the lift-off height. Scatter data of temperature versus mixture fraction [2] show large scatter, with a gradual transition from the inert mixing line to the vigorous flame burning condition. A quantification of a most reactive mixture fraction (η_{mr}) was not attempted.

Numerical methods and model options

The LES and CMC solvers are coupled and the information from CMC (density) is transferred at every time-step of the simulation to the LES in order to update the flow field.

In LES, the convective fluxes of the momentum equation are discretised in a central manner (second order spatial accuracy). In the transport equation for mixture fraction, the convective terms are discretised with a second order accurate total variation diminishing (TVD) scheme. The CMC code is a finite-difference code. Convective transport, term T_1 in eqs. (1) and (2), is discretised with a second-order TVD scheme. The diffusion terms, both in mixture fraction and physical space (T_2 and T_4), are discretised using a second-order accurate central difference scheme. Time step used in simulations is $2.5 \cdot 10^{-7}$.

The boundary conditions for the simulations are given in tab. 1. The detailed chemical mechanism of Li *et al.* [12] is used. The mechanism features 9 species and 19 reversible reactions.

Auto-ignition will not happen for all mixture fractions simultaneously, it will occur at the so called most reactive mixture fraction (η_{mr}). It is defined as a mixture fraction with optimal composition, likely to ignite first. Here, the most reactive mixture fraction is determined with a stand-alone 0D-CMC where the micro-mixing is switched off by using a scalar dissipation rate of 10^{-20} s^{-1}, giving thus a parallel solution to a series of homogeneous reactors of variable mixture fraction. The most reactive mixture fraction as a function of the co-flow temperature is given in tab. 2. It is apparent that the most reactive mixture fraction moves to the rich side as the co-flow temperature is reduced.

Table 2. Most reactive mixture fraction as a function of co-flow temperature for mechanism [12]

T_{cf} [K]	1022	1030	1038	1045	1060	1080
η_{mr} [–]	0.0639	0.0639	0.0587	0.0534	0.0482	0.0482

The computational domain extends axially 30d downstream from the jet inlet (roughly 137 mm, d – nozzle diameter) and radially up to 20d (91.4 mm). Results are obtained with the grid comprising 192 × 48 × 48 cells in LES and 80 × 4 × 4 cells in CMC. The LES grid is stretched smoothly toward the co-flow in the radial direction and is expanded smoothly in the axial direction (y). The jet inlet is resolved with 12 × 12 cells in the inflow (x-z) plane. The CMC grid is expanded smoothly only in the axial direction. The mesh in mixture fraction space consists of 51 nodes, clustered around the most reactive mixture fraction.

In order to generate turbulence in the co-flow, digital filter is used. The co-flow turbulence length-scale was chosen to be 1.6 mm, the size of the holes in the outer disk. The turbulence intensity is 5% [2, 6]. At the inlet of the CMC domain, inert distributions of Q_α are injected. Zero gradient boundary condition is imposed at the sides and the downstream edge of the domain in physical space. In η-space, a Dirichlet boundary condition is used at $\eta = 0$ and $\eta = 1$ and the values of Q_α and Q_T remain there unchanged.

The simulations are started from a developed inert flow field at time t_0. After 20 ms, statistics are collected over a period of 32.5 ms and time averaged data are compared with the measurements. The lift-off height is defined as the location where OH mass fraction reaches $2 \cdot 10^{-4}$ [3].

Results and discussion

Flame structure

First, the results for the conditions as in tab. 1 (T_{cf} = 1045 K) are reported. Figure 1 shows instantaneous OH and HO_2 mass fraction fields at time t_0 + 52.5 ms. The snapshots show turbulent lifted flame with the lift-off height of about 4d. The ignition length of 10d is obtained for a co-flow temperature of 1030 K in the simulations. The uncertainty in the temperature measurements was of the order of 30 K [2] so that use of T_{cf} = 1030 K as inlet boundary condition remains within experimental error. It is clear that HO_2 is generated long before the reaction zone, consistent with its role as an auto-ignition precursor (fig. 1). The highest concentration of HO_2 is found between the most reactive and stoichiometric mixture fraction upstream the flame base in the fuel-lean pre-ignition zone. Some HO_2 survives in the fuel-rich reaction zones of the flame and is depleted in the post flame zones. Subsequently, after build-up of HO_2 generation of OH occurs. The peak OH mass fraction is found around stoichiometric mixture fraction what corresponds also to the high temperature region.

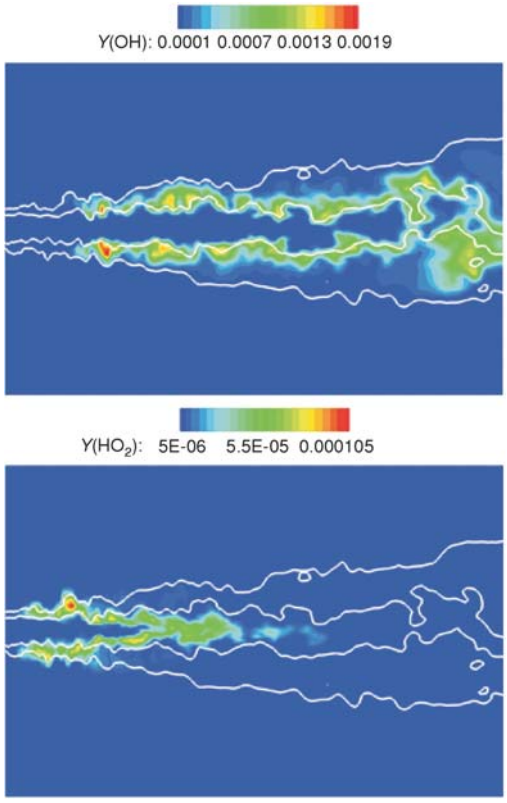

Figure 1. Instantaneous resolved $\widetilde{Y}_{OH}$ and $\widetilde{Y}_{HO_2}$ fields in a symmetry plane (T_{cf} = 1045 K). Inner isoline η_{st}, outer isoline: η_{mr}
(for color image see journal web site**)**

Figure 2 compares centreline profiles of mixture fraction, temperature and the mass fractions of H_2 and H_2O with measurements. The axial mixture fraction profile is in good agreement with the measured values and the penetration of the co-flow towards the axis is well captured. The temperature is slightly higher at the centreline. However this could be expected since the lift-off height is around 4d for co-flow temperature of 1045 K while it is around 10d in the experiments. The earlier reaction can also be seen by the earlier consumption of H_2, and a consistent earlier production of H_2O. The drop in the mean mixture fraction and a slight increase of temperature indicates that the mixing region has reached the centreline ($y \approx 5d$). The high temperature region reaches the axis further downstream ($y > 20d$). Figure 2 also shows that initially the mixing process is dominant and the temperature at the centreline increases slowly. A better understanding of the ignition processes requires examination of the radial profiles, as discussed next.

Figure 3 shows profiles of OH mass fraction and temperature at three different axial stations. The OH radical is a good indicator of the chemistry activity. After occurrence of auto-ignition (at y/d = 10 in experiments), OH concentrations increase by several orders of magnitude – a trend that is well captured by the computations albeit with a shift in the ignition location. The good agreement is observed at the upstream locations (y/d = 11) where the peak and the maxima in the OH mass fraction is captured. However further downstream, OH is under-pre-

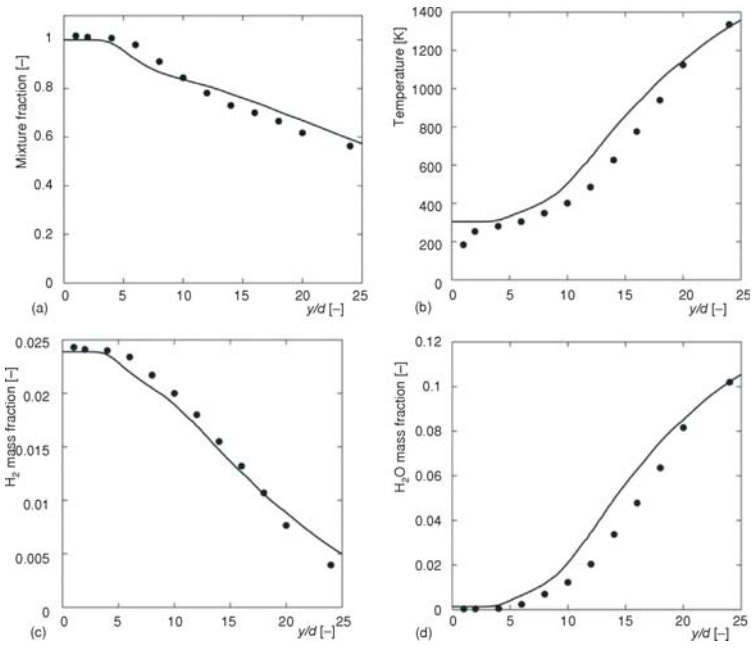

Figure 2. Mixture fraction, temperature and species mass fraction profile along the centreline (T_{cf} = 1045 K). Filled circles: experiments [1, 2]. Lines: present results

dicted (y/d = 14) what might be caused by the under-prediction of the flame lift-off height. As a consequence the mean levels of temperature are over-predicted at y/d = = 11. The other mean profiles are in overall good agreement.

The location of the peak in the calculations is well captured (fig. 3, y/d = 14), meaning that the model predicts the position of the flame at the same radius as observed experimentally. It is clear that the ignition zone is located off the axis at a radial position $r/d \approx 1.3$, *i. e.* on the fuel lean side in the experiments and the current calculations.

These results highlight the potential of the present LES-CMC technique and the codes used to simulate auto-ignition problems which involve complex turbulence-chemistry interactions and to capture intermediate species such as radicals.

Effect of the inlet temperature

The co-flow temperature influences the most lift-off height (H). Several LES-CMC simulations were performed, for a range of a co-flow temperatures (T_{cf} = 1022 K, 1030 K, 1045 K, 1060 K, and 1080 K), in order to assess the trends for the lift-off heights (fig. 4). In fig. 4, the simulation results are compared with the data measured independently by Cabra and Dibble [1], Gordon *et al*. [5] and Wu *et al.* [18]. The Gordon *et al.* [5] results (a) and (b) indicate measurements taken from two separate experiments. In the simulations, the flame with T_{cf} = 1080 K is an attached flame. When the temperature is reduced, a lifted flame is observed. The results confirm previous findings with transported PDF simulations [3]. In their calculations a lift-off height of H/d = 10 corresponded to a co-flow temperature of 1033 K.

As mentioned above, the uncertainty in the temperature measurements [2] was of the order of 30 K, as indicated by the horizontal error bar in fig. 4. It is clear that the lift-off height for T_{cf} = 1045K is different but the result with T_{cf} = 1030 K, which is still within the experimental uncertainty, matches measurements of [2] very well (H/d = 9.7). Due to the high sensitivity of the lift-off height to the co-flow temperature it is hard to obtain absolute agreement with the measurements. However, the simulation results are in good agreement with the measurements of [18].

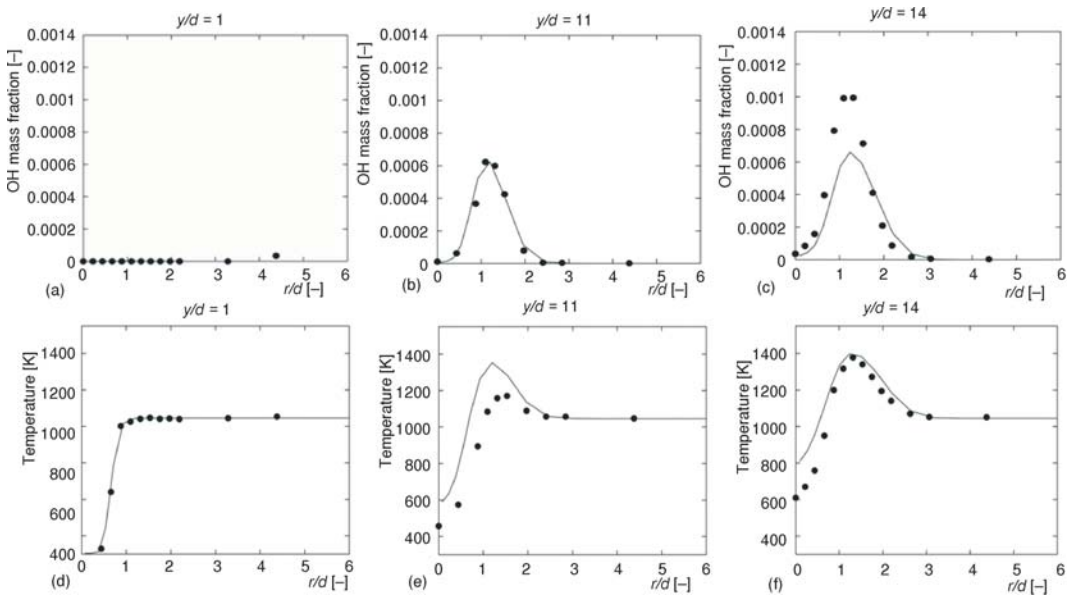

Figure 3. Radial profiles of mean OH mass fraction and temperature at three axial stations (T_{cf} = 1045 K). Filled circles: experiments [1, 2]. Lines: present results

High sensitivity of the lift-off height to the inlet temperature (fig. 4) suggests as well that flames with the same lift-off height rather than the same co-flow temperature should be selected for comparison with the measurements. Therefore, radial profiles at different axial locations for T_{cf} = 1030 K are compared with measurements at conditions listed in tab. 1 (fig. 5).

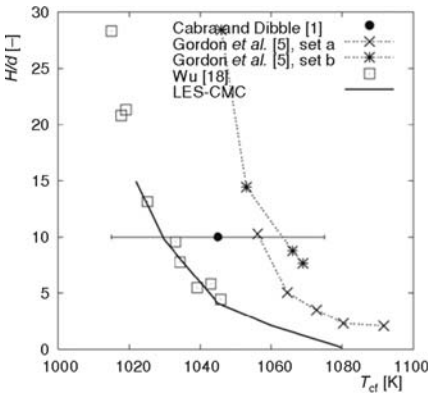

Figure 4. Lift-off height as a function of the co-flow temperature

Radial profiles of the OH mass fractions are shown in fig. 5. Now, the presence of ignition is well predicted. The quantitative agreement is good, although, in the calculations, the maximum OH concentration is shifted toward the co-flow region. Further downstream at y/d = 14, the OH peak is well captured.

The conclusion here is that, with the LES-CMC code, good agreement with experimental data is obtained, provided the co-flow temperature is chosen appropriately.

Flame stabilization mechanisms

The stabilisation of the lifted flames can be governed by various mechanisms. Typically, two competing mechanisms dominate the stabilisation: auto-ignition and premixed flame propagation. Stabilisation mechanisms of the lifted flames have received a lot of attention lately due to its great importance in industry.

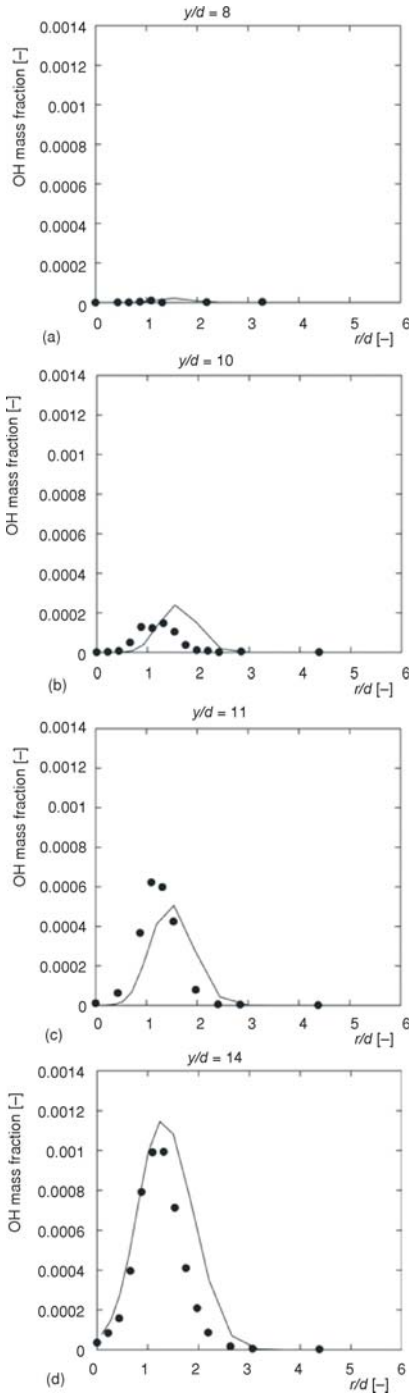

Figure 5. Radial profiles of mean OH mass fraction at four axial stations. Filled circles: experiments [1, 2]. Lines: present results for T_{cf} = 1030 K

RANS-type simulations [3, 5, 8] and LES [10, 11] have analyzed the lifted flame of [2] in order to determine stabilisation mechanism. The goal of all these studies was to answer to the original uncertainty of [2], namely if this flame is stabilised by auto-ignition or premixed flame propagation. There is no consensus in the literature at the moment.

The analysis of a time history of the radical concentrations or the convection-diffusion-reaction (CDR) budgets, *i. e*. the analysis of each term in the CMC transport equations, can aid the identification of the dominant flame stabilisation mechanism, as suggested in [5]. Following [5], the flame will be stabilised by auto-ignition if the HO_2 radical builds up prior to the build-up of H, O, and OH and if CDR budgets show a convection-reaction balance. On the other hand, if the mass fractions of all the radicals begin increasing at the same point, the flame is stabilised by premixed flame propagation. In this case, a convection-diffusion balance is present at the locations upstream of the flame base, with the chemistry term relatively small. In the reaction zone, there should be a balance between diffusion and reaction.

Figure 6 shows instantaneous resolved OH and HO_2 fields in a symmetry plane for two co-flow temperatures (1030 K and 1060 K). With the co-flow temperature T_{cf} = 1030 K, it is clear that HO_2 is generated long before the flame stabilisation point is reached. Also, it is apparent that it starts to be consumed as soon as the production of OH begins. This build-up of the HO_2 radical upstream the flame base, prior to ignition, is one of the indicators of the auto-ignition stabilisation of the flame. For T_{cf} = 1060 K, show the HO_2 radical build up very close to the injector, less than 2*d* upstream of the generation of OH. The concentration of the HO_2 radical is also much lower than for the cases with lower co-flow temperatures. As can be seen in fig. 4, for higher co-flow temperatures, the lift-off height also becomes less sensitive to the changes in the co-flow temperature. This makes it unclear if the flame is still stabilised by auto-ignition, with short ignition delay time, since the high co-flow temperature is accelerating the reactive processes. In order to assess the stabilization mechanism in this situation the balance of the terms in the CMC eq. (2) has to be examined. This has been done, in [19], where the averaged contribution of each term is plotted at four

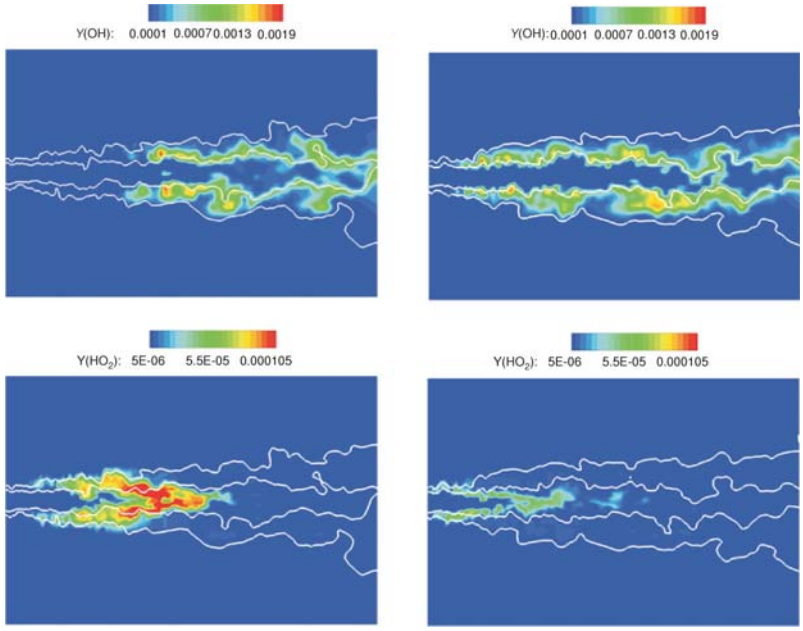

Figure 6. Instantaneous resolved $\widetilde{Y}_{OH}$ and $\widetilde{Y}_{HO_2}$ fields in a symmetry plane. Left: T_{cf} = 1030 K. Right: T_{cf} = 1060 K. Inner isoline: η_{st}, outer isoline: η_{mr} (for color image see journal web site)

different axial locations covering the pre-ignition region (upstream of the flame base), the flame base and the region downstream of the flame base. Similar behaviour is observed for above examined temperatures. It was shown that the diffusion in physical space is negligible what confirms that the flames are stabilized by auto-ignition. At the flame base, the chemical source term is a few orders of magnitudes higher than at the other locations. It is mainly in balance with the convection, but the scalar dissipation rate term is important as well.

Moreover, the observations are in agreement with the findings of [5] where the Berkeley case was examined applying above mentioned indicators for the determination of the stabilisation mechanism. In the RANS-CMC calculations of [8], for the 1025 K case, the lift-off height was reported to be controlled by premixed flame propagation, where strong axial diffusion and a weak chemical term were found upstream the flame base. For the 1080 K case, the auto-ignition was suggested as controlling mechanism in [8].

Conclusions

The numerical investigation of a lifted turbulent hydrogen jet flame in a co-flow of hot, vitiated air was presented.

The LES-CMC approach with detailed chemical mechanism was able to reproduce the experimentally measured axial and radial profiles of mixture fraction, temperature and major species very well. In the calculations, the best agreement was obtained for the co-flow temperature of 1030 K, which is within experimental uncertainties. Good agreement of species mass fraction radial profiles is obtained when the lift-off height is correct.

The flame is stabilized by auto-ignition. No evidence of premixed flame propagation is found: the diffusion in physical space is negligible for all studied conditions. Upstream of the

flame base, a clear convection-reaction balance was observed, with the scalar dissipation being important as well. Inside the reactive zone, the scalar dissipation rate is dominant in balancing the chemistry, approaching the well-known structure of a non-premixed flame. HO_2, as a key intermediate species, is formed well before the flame stabilisation point, consistent with its role as auto-ignition precursor.

References

[1] Cabra, R., Dibble, R. W., Lifted CH4/Air Jet Flame in a Vitiated co-Flow, http://www.me.berkeley.edu/cal/vcb/data/ VCHNData.html.
[2] Cabra, R., *et al*., Simultaneous Laser Raman-Rayleigh-Lif Measurements and Numerical Modeling Results of a Lifted Turbulent H_2/N_2 Jet Flame in a Vitiated Co-Flow, 29th Symposium on Combustion Sapporo, Japan, 2003, *Proceedings*, The Combustion Institute, Pittsburgh, Penn., USA, 2003, pp. 1881-1888
[3] Cao, R. R., *et al.*, Turbulent Lifted Flames in a Vitiated Co-Flow Investigated Using Joint PDF Calculations, *Combust. Flame, 142* (2005), 4, pp. 438-453
[4] Gkagkas, K., Lindstedt, R. P., The Impact of Reduced Chemistry on Auto-Ignition of H_2 in Turbulent Flows, *Combust. Theory Model., 13* (2009), 4, pp. 607-643
[5] Gordon, R. L., *et al.*, A Numerical Study of Auto-Ignition in Turbulent Lifted Flames Issuing into Vitiated Co-Flow, *Combust. Theory Model., 11* (2007), 3, pp. 351-376
[6] Masri, A. R., *et al.*, PDF Calculations of Turbulent Lifted Flames of H_2/N_2 Fuel Issuing into a Vitiated Co-Flow, *Combust. Theory Model., 8* (2003), 1, pp. 1-22
[7] Myhrvold, T., *et al*., A Numerical Investigation of a Lifted H_2/N_2 Turbulent Jet Flame in a Vitiated Co-Flow, *Combust. Sci. Technol., 178* (2009), 6, pp. 1001-1030
[8] Patwardhan, S. S., *et al*., CMC Simulations of Lifted Turbulent Jet Flames in a Vitiated Co-Flow, *Proc. Combust. Inst., 32* (2009), 2, pp. 1705-1712
[9] Duwig, C., Fuchs, L., Large Eddy Simulation of a H_2/N_2 Lifted Flame in a Vitiated Co-Flow, *Combust. Sci. Technol., 180* (2008), pp. 453-480
[10] Navarro-Martinez, S., Kronenburg, A., Flame Stabilization Mechanisms in Lifted Flames, *Flow Turbl. Combust., 87* (2011), 2-3, pp. 377-406
[11] Jones, W. P., Navarro-Martinez, S., Large Eddy Simulation of Auto-Ignition with a Subgrid Probability Density Function Method, *Combust. Flame, 150* (2007), 3, pp. 170-187
[12] Li, J., *et al.*, An Updated Comprehensive Kinetic Model of Hydrogen Combustion, *Inter. J. Chem. Kinet., 36* (2004), 10, pp. 566-575
[13] Stanković, I., *et al.*, Simulation of Hydrogen Auto-Ignition in a Turbulent Co-Flow of Heated Air with LES and CMC Approach, *Flow Turb. Combust., 86* (2011), 3-4, pp. 689-710
[14] Pierce, C. D., Moin, P., A Dynamic Model for Subgrid-Scale Variance and Dissipation Rate of a Conserved Scalar, *Phys. Fluids, 10* (1998), 12, pp. 3041-3044
[15] Triantafyllidis, A., *et al*., Large Eddy Simulations of Forced Ignition of a Non-Premixed Bluff-Body Methane Flame with Conditional Moment Closure, *Combust. Flame, 156* (2009), 12, pp. 2328-2345
[16] O'Brien, E. E., Jiang, T. L., The Conditional Dissipation Rate of an Initially Binary Scalar in Homogeneous Turbulence, *Phys. Fluids, 3* (1991), 12, pp. 3121-3123
[17] Navarro-Martinez, S., *et al*., Conditional Moment Closure for Large Eddy Simulations, *Flow Turbul. Combust., 75* (2005), 1-4, pp. 245-274
[18] Wu, Z., *et al*., Lift-off Heights of Turbulent H_2/N_2 Jet Flames in a Vitiated Co-Flow, *Proceedings*, Australian Symposium on Combustion and the Eighth Australian Flame Days, The Combustion Institute, Melbourne, Australia, 2003
[19] Stanković, I., Merci, B., LES-CMC Simulations of Turbulent Hydrogen Flame in a Vitiated Air Co-Flow, *Proceedings*, 7th Mediterranean Combustion Symposium, Sardinia, Italy, 2011

Paper submitted: July 4, 2012
Paper revised: March 21, 2013
Paper accepted: March 22, 2013